

(NASA-CR-153407) NOVEL DUPLEX  
VAPOE-ELECTROCHEMICAL METHOD FOR SILICON  
SOLAR CELLS Quarterly Progress Report,  
1 Feb. - 30 Apr. 1977 (Stanford Univ.) 36 p  
HC AC3/MF A01  
N77-30607  
Unclas  
41992  
CSCL 10A G3/44

ERDA/JPL 954471-77/2  
Distribution Category UC-63

Quarterly Progress Report No. 5  
Covering the period February 1, 1977 to April 30, 1977

NOVEL DUPLEX VAPOR-ELECTROCHEMICAL METHOD FOR  
SILICON SOLAR CELLS

By: Vijay K. Kapur, L. Nanis, and Angel Sanjurjo

Prepared for:

JET PROPULSION LABORATORY  
California Institute of Technology  
4800 Oak Grove Drive  
Pasadena, CA 91103

Attn: Dr. Ralph Lutwack  
Spacecraft Power Station

Contract No. 954471 under NAS 7-100  
SRI Project PYU 4980



STANFORD RESEARCH INSTITUTE  
Menlo Park, California 94025 · U.S.A.





STANFORD RESEARCH INSTITUTE  
Menlo Park, California 94025 · U.S.A.

ERDA/JPL 954471-77/2  
Distribution Category UC-63

July 1977

Quarterly Progress Report No. 5  
Covering the period February 1, 1977 to April 30, 1977

NOVEL DUPLEX VAPOR-ELECTROCHEMICAL METHOD FOR  
SILICON SOLAR CELLS

By: Vijay K. Kapur, Leonard Nanis, and Angel Sanjurjo

Prepared for:

JET PROPULSION LABORATORY  
California Institute of Technology  
4800 Oak Grove Drive  
Pasadena, California 91103

Attention: Dr. Ralph Lutwack  
Spacecraft Power Station

Contract No. 955471 under NAS 7-100  
SRI Project PYU 4980

STANFORD RESEARCH INTERNATIONAL  
Menlo Park, California 94025 U.S.A.

**This work was performed for the Jet Propulsion Laboratory, California Institute of Technology, under NASA Contract NAS7-100 for the U.S. Energy Research and Development Administration, Division of Solar Energy.**

**The JPL Low-Cost Silicon Solar Array Project is funded by ERDA and forms part of the ERDA Photovoltaic Conversion Program to initiate a major effort toward the development of low-cost solar arrays.**

#### ACKNOWLEDGEMENTS

The assistance of Drs. D. Hildenbrand, K. Lau and P. Kleinschmidt for obtaining the data on the thermal decomposition of  $\text{Na}_2\text{SiF}_6$  and for the impurity analysis of  $\text{SiF}_4$  gas by mass spectrometry is gratefully acknowledged.

## SUMMARY

Silicon was produced by alternate pulse feeding of the reactants  $\text{SiF}_4$  gas and liquid sodium. The average temperature in the reactor could be controlled to within  $\pm 20^\circ\text{C}$  in the temperature range  $400\text{--}600^\circ\text{C}$ , by regulating the amount of reactant in each pulse. Batches of reaction product ( $\text{NaF}$ ,  $\text{Na}_2\text{SiF}_6$ ,  $\text{Si}$ ) as large as 250 g, containing 25 to 30 g of silicon, were prepared by the alternate pulse feeding technique.

Silicon tetrafluoride gas was analyzed by mass spectrometry to determine the nature and amount of contained volatile impurities. The major impurities were found to be silicon oxyfluorides ( $\approx 4.0\%$ ), sulfur oxyfluorides ( $\approx 0.1\%$ ), and sulfur dioxide (0.05%). Sodium metal was analyzed by emission spectrography, and it was found to contain only calcium (100 ppm wt) and copper (8 ppm wt) as impurities.

The decomposition of  $\text{Na}_2\text{SiF}_6$  to  $\text{NaF}$  and  $\text{SiF}_4$  was studied by an effusion method to determine the equilibrium pressure of  $\text{SiF}_4$  at temperatures ranging from 585 to 650 K ( $312$  to  $377^\circ\text{C}$ ).

## CONTENTS

ACKNOWLEDGEMENTS . . . . .	ii
SUMMARY . . . . .	iii
LIST OF ILLUSTRATIONS . . . . .	v
TABLE . . . . .	v
INTRODUCTION . . . . .	1
SODIUM PULSE FEEDER . . . . .	4
PULSE FEEDING OF REACTANTS . . . . .	6
PULSE FEEDING OF SiF <sub>4</sub> GAS ONLY (MONOPULSING) . . . . .	10
PULSE FEEDING OF LIQUID SODIUM AND SiF <sub>4</sub> GAS (BIPULSING). . . . .	12
ANALYSIS OF SILICON TETRAFLUORIDE BY MASS SPECTROMETRY . . . . .	16
Experimental . . . . .	16
Results . . . . .	17
Discussion and Conclusions . . . . .	18
ANALYSIS OF SODIUM METAL BY EMISSION SPECTROGRAPHY . . . . .	20
DISSOCIATION PRESSURE AND THERMODYNAMIC STABILITY OF Na <sub>2</sub> SiF <sub>6</sub> (c) . . . . .	21
FUTURE WORK . . . . .	27
REFERENCES . . . . .	28

## ILLUSTRATIONS

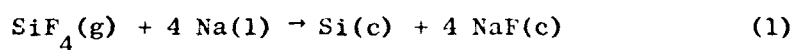
1.	Sodium Feeder . . . . .	5
2.	Apparatus for SiF <sub>4</sub> -Na Reaction . . . . .	7
3.	SiF <sub>4</sub> Pressure and Reaction Temperature Versus Time (monopulsing) . . . . .	9
4.	Monopulsing, SiF <sub>4</sub> Pressure Versus Time (Schematic) . . . . .	10
5.	SiF <sub>4</sub> Pressure and Reaction Temperature Versus Time (Bipulsing) . . . . .	13
6.	Bipulsing-SiF <sub>4</sub> Pressure Versus Time (Schematic) . . . . .	14
7.	Torsion Effusion Measurements of P <sub>SiF<sub>4</sub></sub> . . . . .	23
8.	Equilibrium Pressure of SiF <sub>4</sub> Versus Temperature . . . . .	25

## TABLE

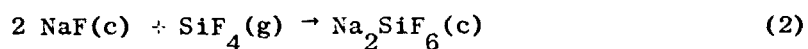
1.	Mass Spectrometric Analysis of Commercial SiF <sub>4</sub> . . . . .	19
----	--	----

## INTRODUCTION

At SRI International, silicon has been produced by the reduction of  $\text{SiF}_4$  gas with liquid sodium<sup>1,2</sup> according to the reaction



In a side reaction, sodium fluosilicate ( $\text{Na}_2\text{SiF}_6$ ) is also produced<sup>3</sup> from the reaction of NaF with  $\text{SiF}_4$  according to

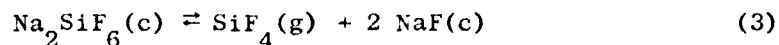


The reaction products, therefore, consist of Si, NaF and  $\text{Na}_2\text{SiF}_6$ . The  $\text{SiF}_4$  - Na reaction (Equation 1) is performed in a reaction kettle<sup>4</sup> by providing an atmosphere of  $\text{SiF}_4$  gas over the surface of liquid sodium. The reaction kettle is heated to about 200°C in order to initiate the reaction shown in Equation 1. Once the reaction has started, a large amount of heat is liberated, which speeds the reaction to completion. However, in a simplified consideration, as the reaction proceeds, the solid reaction products Si, NaF and  $\text{Na}_2\text{SiF}_6$  cover the surface of the liquid sodium, thus decreasing the accessibility of  $\text{SiF}_4$  gas. For the reaction to continue further,  $\text{SiF}_4$  gas has to diffuse through an increasingly thick layer of reaction products to reach clean sodium. It is postulated that, after a while, the surface of the liquid sodium becomes so heavily coated with reaction products that a diffusion limitation of the reaction is established, which is controlled by the thickness and the porosity of the product layer, as well as by temperature and pressure of  $\text{SiF}_4$ . As a consequence, some unreacted sodium is

left buried in the reaction products. The presence of sodium metal in the reaction products is undesirable because it reacts vigorously with HCl solutions used for leaching out the sodium fluorides. Of course, the acid leachout is itself desirable, because, with water as leachant, alkaline solution is formed, which causes the unwanted dissolution of silicon. To minimize the amount of unreacted sodium in the reaction products, it was decided to perform the  $\text{SiF}_4$ -Na reaction (Equation 1) by alternately pulse feeding the reactants in the sequence: liquid sodium pulse followed by  $\text{SiF}_4$  gas pulse.

The pulse feeding technique used for the  $\text{SiF}_4$ -Na reaction is described in the following section of this report. To pinpoint possible sources of impurity pickup, we analyzed both the  $\text{SiF}_4$  gas and the sodium metal used in the reaction (1).  $\text{SiF}_4$  gas is known to contain oxygen and sulfur dioxide as impurities, but to check for possible contamination of volatile metal halides,  $\text{SiF}_4$  gas was analyzed by mass spectrometry. Sodium metal also was analyzed by emission spectrography. The results of these analyses are discussed in this report.

Because of the importance of sodium fluosilicate to this project, both as a reaction product (Equation 1,2) and as a possible intermediate material for  $\text{SiF}_4$  generation, a study was undertaken to determine the equilibrium partial pressure of  $\text{SiF}_4$ (g) above  $\text{Na}_2\text{SiF}_6$ (c) and its decomposition products  $\text{SiF}_4$ (g) and  $\text{NaF}$ (c). Data available in the literature are widely different for the reaction which is the reverse of Equation 2, namely



The compound  $\text{Na}_2\text{SiF}_6$  has been detected as a product of the reaction between Na and  $\text{SiF}_4$ . Since silicon is the desired product, experiments

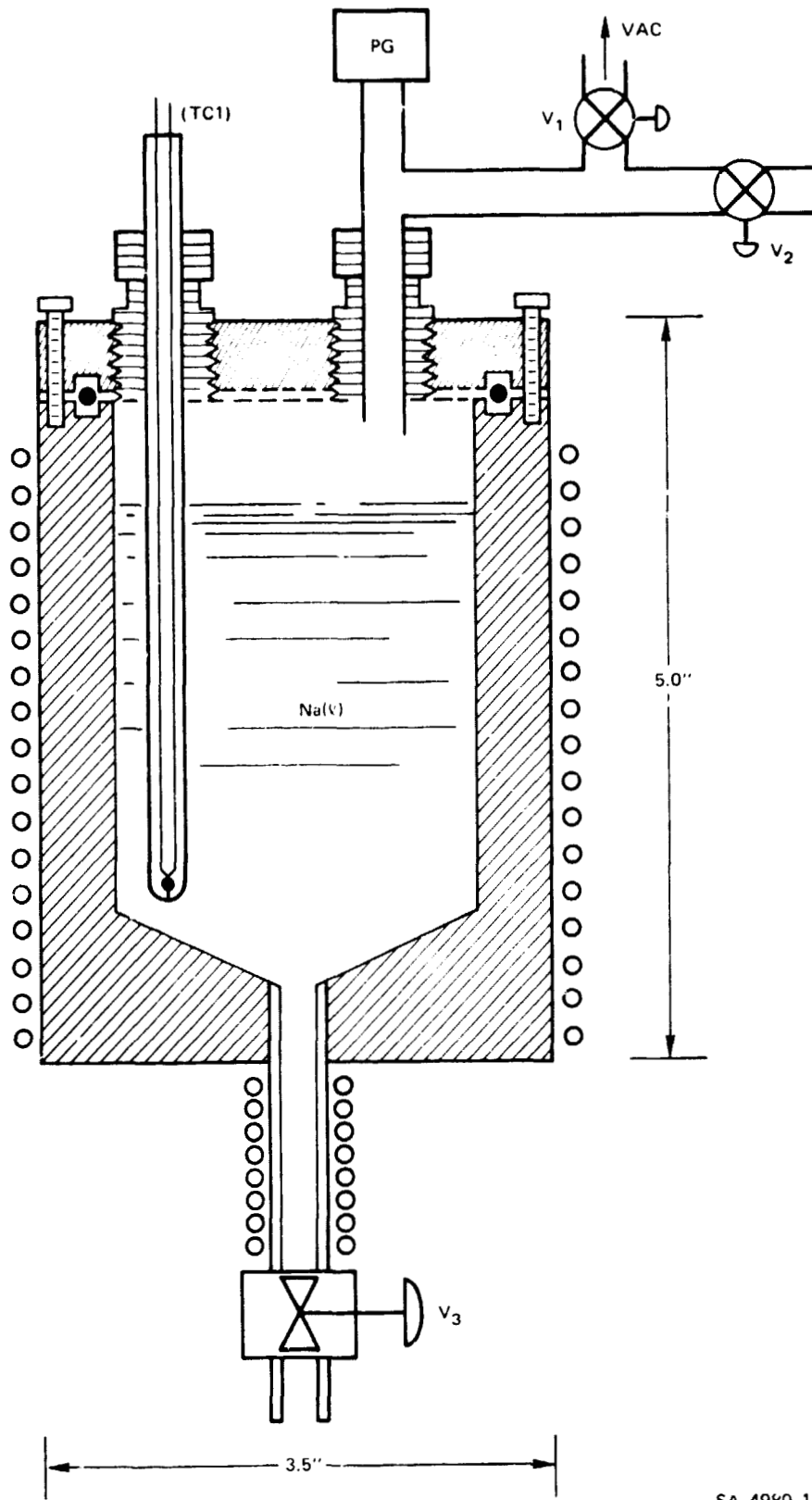
to minimize the formation of  $\text{Na}_2\text{SiF}_6$  are in progress. It is expected that an increase in reaction temperature will hasten the decomposition of  $\text{Na}_2\text{SiF}_6$ . The alternate pulse feed method is being used to control reaction temperature. However, the lowest possible temperature is desirable in order to decrease impurity pickup from container materials.

Alternatively, a silicon purification scheme is also possible in which the product silicon is anodically dissolved in a fluoride melt and cathodically deposited to accomplish electrolytic refining, utilizing  $\text{Na}_2\text{SiF}_6$  and  $\text{NaF}$  to form a suitable molten electrolyte. In this case, conditions for the reactor operation might be controlled so as to encourage the formation of  $\text{Na}_2\text{SiF}_6$  during the reduction of  $\text{SiF}_4$  by Na.

The decomposition of  $\text{Na}_2\text{SiF}_6$  takes on added significance as a source of  $\text{SiF}_4$  for reaction with Na, because inexpensive sources of silicon ( $\text{H}_2\text{SiF}_6$ ) may be used to form  $\text{Na}_2\text{SiF}_6$ . Members of the Thermochemistry Group in our Materials Research Center (D. Hildenbrand, K. Lau) performed the effusion vapor pressure measurements presented in this report, which establish the temperature-pressure relationship for  $\text{SiF}_4$  for the reaction in Equation 3.

## SODIUM PULSE FEEDER

To introduce pulses of liquid sodium into the reaction kettle, we constructed a sodium pulse feeder (Fig. 1) from a cylindrical stainless steel container,  $5\frac{1}{2}$  inches long, 3 inches in diameter, with  $\frac{1}{2}$  inch thick walls. The top of the feeder is closed by bolting on a stainless steel lid with an O-ring seal. A thermocouple (TC1), inserted through the lid, is used to measure the temperature of liquid sodium. The sodium feeder can be evacuated through a needle valve ( $V_1$ ) and it can also be filled with an inert gas through another needle valve ( $V_2$ ). The pressure gauge (PG) is used to measure the back-up pressure of the inert gas in the feeder. The inside floor of the feeder is conically tapered to assist the flow of liquid sodium. A hole in the center of the floor connects to a welded stainless steel tube ( $\frac{3}{8}$  in O.D.), through which liquid sodium is drawn out. The capacity of the sodium feeder is about 300 ml and it can easily contain 250 g of sodium. The outflow of liquid sodium can be regulated by a stainless steel bellows valve  $V_3$ .



SA-4980-15

FIGURE 1 SODIUM FEEDER

## PULSE FEEDING OF REACTANTS

To perform the  $\text{SiF}_4$ -Na reaction by pulse feeding the reactants, we connected the reaction kettle (described in Quarterly Progress Report 2 and 3) to the sodium pulse feeder containing liquid sodium and also to the  $\text{SiF}_4$  storage through a pre-reservoir of  $\text{SiF}_4$  gas, as shown in Fig. 2. The reaction kettle (c) was first evacuated via a needle valve,  $V_6$ . To perform the  $\text{SiF}_4$ -Na reaction (Equation 1), we introduced pulses of liquid sodium and  $\text{SiF}_4$  gas by opening valves  $V_3$  and  $V_4$  as required. During the reaction, the pressure of  $\text{SiF}_4$  gas in the system, measured by the pressure transducer (PT), and the average reaction temperature, measured by the thermocouple (TC2), were continuously recorded.

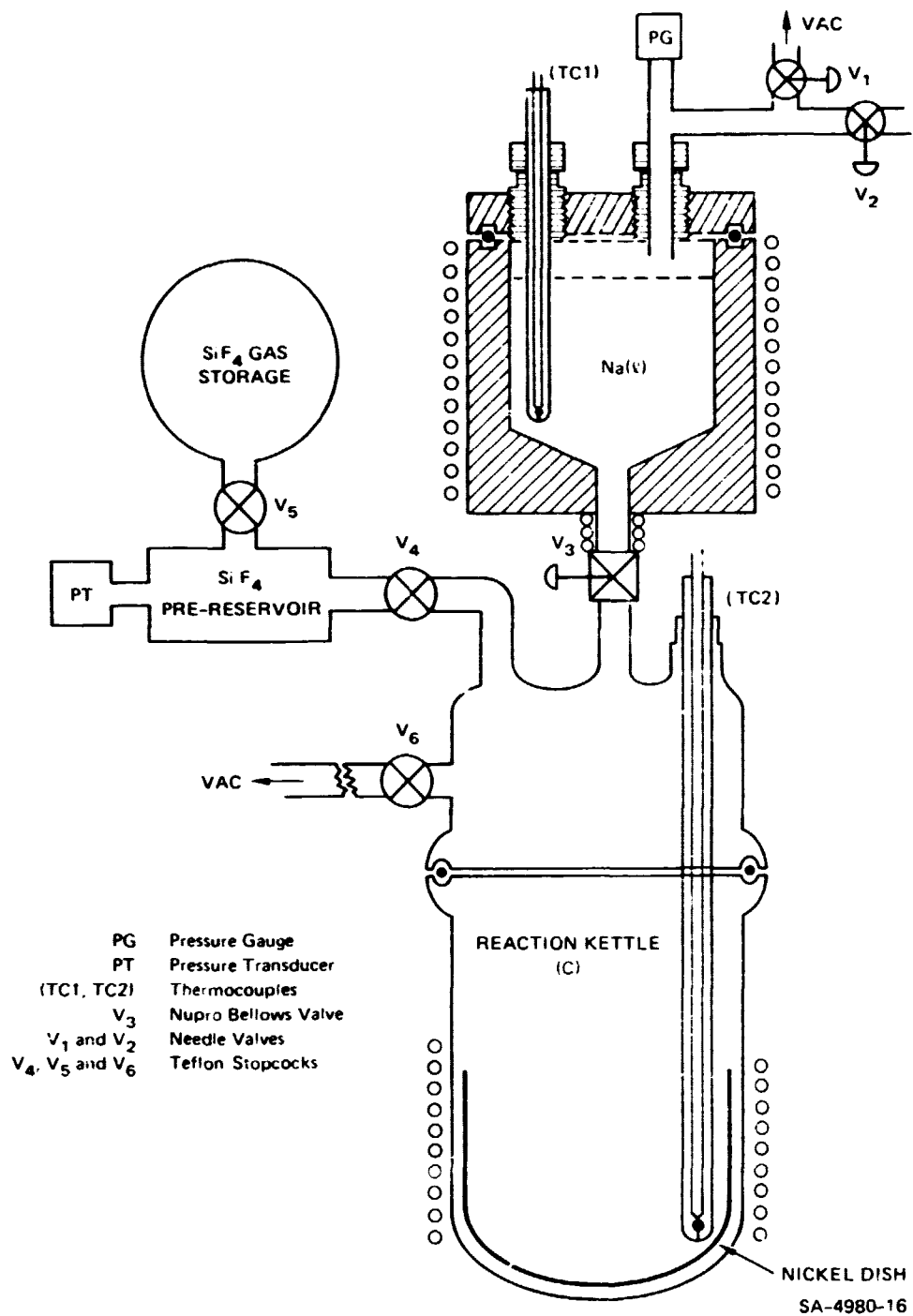


FIGURE 2 APPARATUS FOR SiF<sub>4</sub> — Na REACTION

### PULSE FEEDING OF $\text{SiF}_4$ GAS ONLY (MONOPULSING)

In our first attempt to use the pulse feeding technique, only  $\text{SiF}_4$  gas was pulse fed over a pool of liquid sodium. To start the experiment, we first evacuated the reaction kettle (C, Fig. 2) and introduced liquid sodium (12.08 g) from the sodium feeder by opening the bellows valve,  $V_3$  (Fig. 2). As shown in the temperature trace of Fig. 3, sodium was further heated at  $305^\circ\text{C}$  (a temperature well above the initiation temperature of the  $\text{Na-SiF}_4$  reaction) before pulses of  $\text{SiF}_4$  gas were fed into the reaction kettle.  $\text{SiF}_4$  gas pulses were introduced by opening stopcock  $V_4$  (Fig. 2) connecting the reaction kettle to the  $\text{SiF}_4$  gas pre-reservoir. Pressure in the system was measured by a pressure transducer (PT) connected to the  $\text{SiF}_4$  gas pre-reservoir. Traces of the pressure and temperature of a typical monopulse experiment are shown in Fig. 3. The trace of  $\text{SiF}_4$  pressure recorded against time can be divided into four time intervals, as shown schematically in Fig. 4.

During the time interval  $t_1$ , the  $\text{SiF}_4$  pre-reservoir was filled with  $\text{SiF}_4$  gas and was kept isolated from the reaction kettle containing liquid sodium. The pressure transducer showed the pressure in the pre-reservoir increasing to  $P_1$ . Towards the end of the holding period,  $t_2$ , the stopcock  $V_4$  (Fig. 2) was opened and a pulse of  $\text{SiF}_4$  gas was introduced into the reaction kettle. Because of the larger volume of lines and container now available to  $\text{SiF}_4$  gas, its pressure suddenly dropped from  $P_1$  to  $P_2$  during the brief time interval  $t_3$ . Since the sodium metal was already at  $305^\circ\text{C}$ , the  $\text{SiF}_4\text{-Na}$  reaction started instantaneously and consumed  $\text{SiF}_4$  gas, causing a further slower drop of  $P_{\text{SiF}_4}$  from  $P_2$  to vacuum. During the time interval  $t_4$ ,  $P_{\text{SiF}_4}$  decreased as

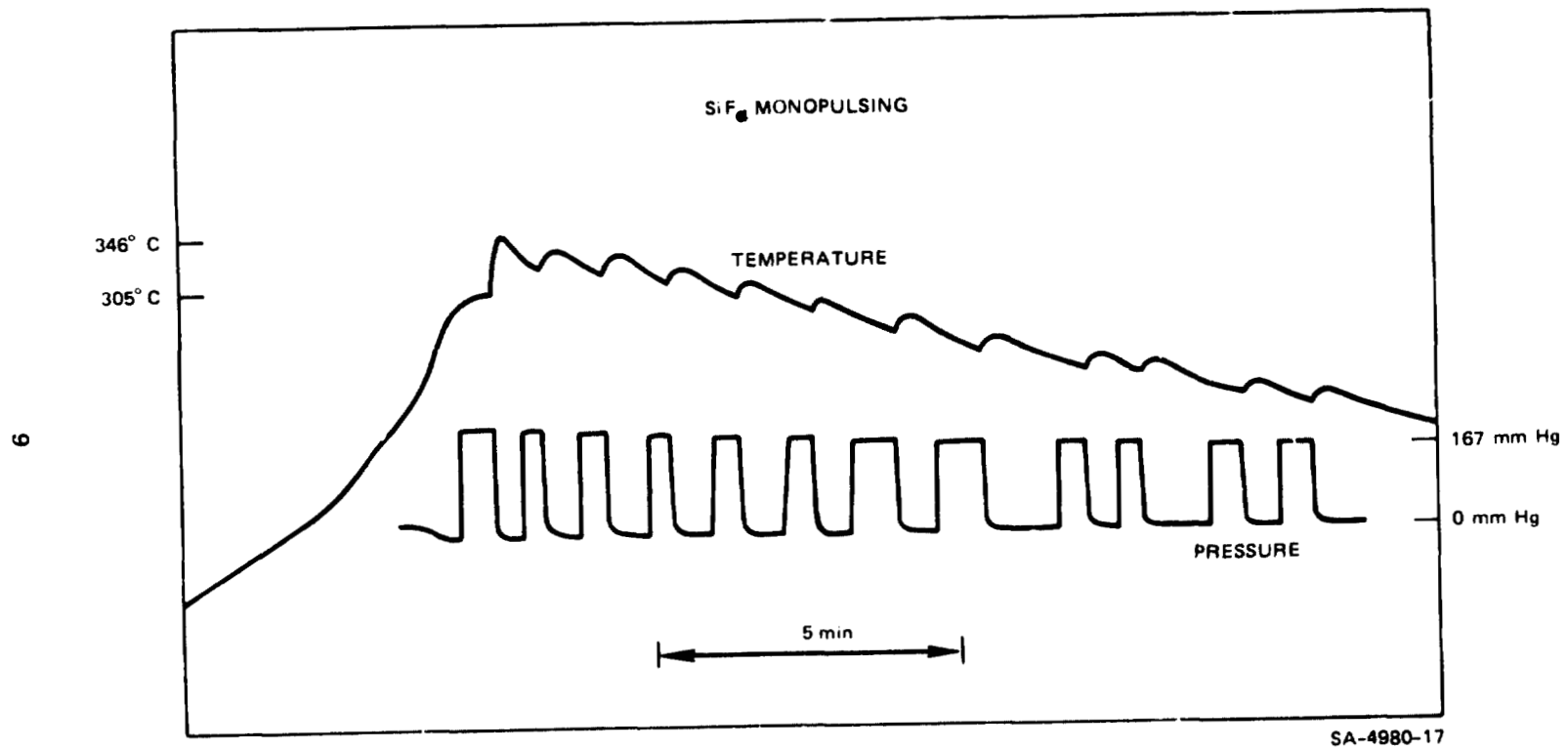


FIGURE 3 SiF<sub>4</sub> PRESSURE AND REACTION TEMPERATURE VERSUS TIME (MONOPULSING)

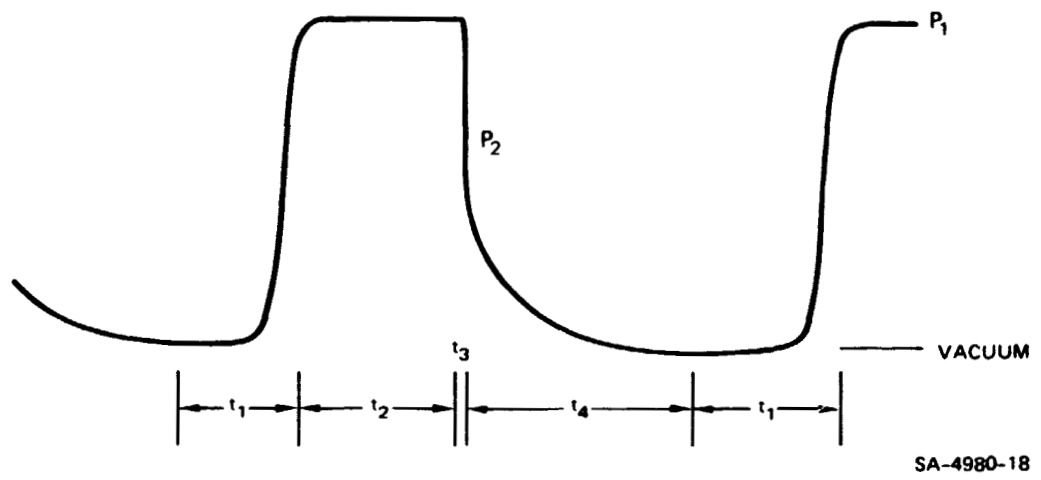


FIGURE 4 MONOPULSING  $\text{SiF}_4$  PRESSURE VERSUS TIME (SCHEMATIC)

controlled by the kinetics of the reaction. As each pulse of  $\text{SiF}_4$  gas reacted with Na, the heat of the reaction produced a corresponding increase in the reaction temperature, as observed in the temperature trace shown in Fig. 3. Following reaction, the kettle was again disconnected from the  $\text{SiF}_4$  pre-reservoir by closing the stopcock  $V_4$ , thus again commencing the cycle shown in Fig. 4. After a few pulses of  $\text{SiF}_4$  had been fed, the reaction products covered the surface of the liquid sodium. When the introduction of an  $\text{SiF}_4$  pulse produced no corresponding increase in reaction temperature, it was assumed that all of the available sodium had reacted.

Substantial amounts of unreacted sodium (greater than 20%) were found in the reaction products of monopulsing experiments. Therefore, we adopted a procedure for pulse feeding both  $\text{SiF}_4$  gas and liquid sodium (bipulsing). The sodium feeder described above (Fig. 1) was used in bipulsing experiments.

## PULSE FEEDING OF LIQUID SODIUM AND $\text{SiF}_4$ GAS (bipulsing)

Liquid sodium and  $\text{SiF}_4$  gas were both pulse fed into the reaction kettle to avoid carrying over unreacted sodium in the reaction products. Typical pressure and temperature recordings are shown in Fig. 5. Every pulse of sodium added a fresh layer of sodium on top of the existing reaction products so that the following pulse of incoming  $\text{SiF}_4$  gas directly contacted liquid sodium. The average amount of liquid sodium in each pulse was 3 g and each sodium pulse was followed by 8 to 10 pulses of  $\text{SiF}_4$  gas to produce complete reaction. The  $\text{SiF}_4$  pulses were fed directly into the reaction kettle, without going through the intermediate step of filling the pre-reservoir (as in monopulsing experiments). During the course of reaction following a pulse, the pressure of  $\text{SiF}_4$  in the reaction kettle decreased from a maximum of 580 mm Hg to vacuum. For each pulse of  $\text{SiF}_4$ , a rapid pressure increase was followed by the exponential decay of  $P_{\text{SiF}_4}$  due to the  $\text{SiF}_4$ -Na reaction, as shown in enlarged detail in Fig. 6. An average temperature of  $600^\circ\text{C}$  was maintained for the reaction whose history is partly shown in Fig. 5.

An extremely useful feature of the bipulsing technique is that the average temperature inside the reactor can be maintained nearly constant by regulating the amounts of sodium and  $\text{SiF}_4$  in each pulse. Since the temperature was held constant by reaction control, it could not serve as an indicator of the complete consumption of sodium in the  $\text{SiF}_4$ -Na reaction, as was possible in the monopulsing mode. It was assumed that about 8 to 10 pulses of  $\text{SiF}_4$  were enough to completely react with an average sodium pulse amount of 3 g. After feeding about 10 pulses of  $\text{SiF}_4$  gas, we fed another pulse of liquid sodium (Fig. 5) and then repeated the  $\text{SiF}_4$  pulsing process. Batches of reaction products weighing 250 g,

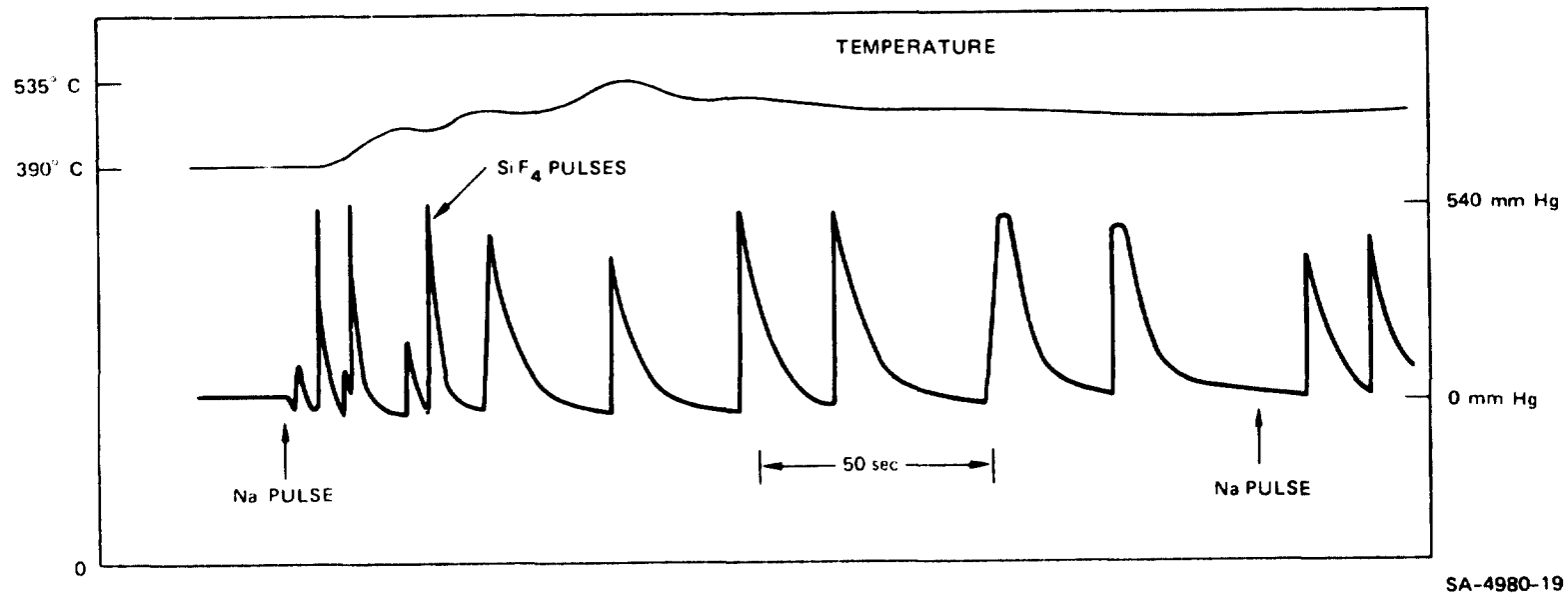
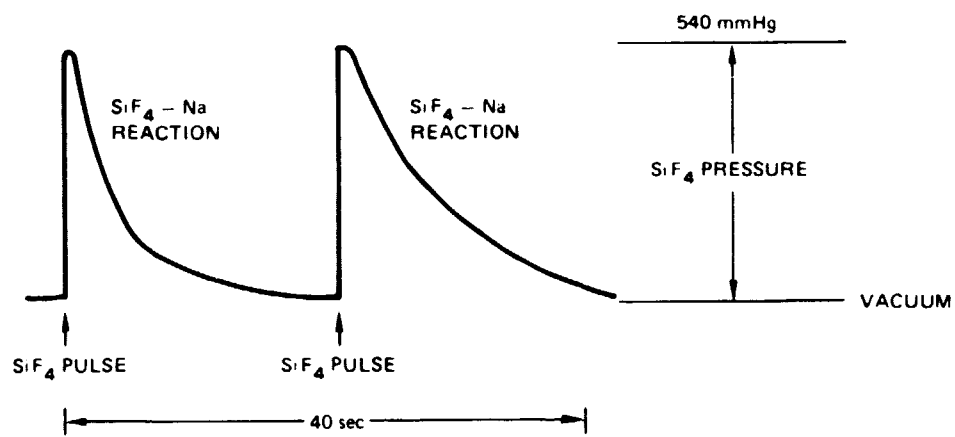


FIGURE 5  $\text{SiF}_4$  PRESSURE AND REACTION TEMPERATURE VERSUS TIME (BIPULSING)



SA-4980-20

FIGURE 6 BIPULSING -  $\text{SiF}_4$  PRESSURE VERSUS TIME (SCHEMATIC)

and containing 25 to 30 g of silicon, were produced. The amount of unreacted sodium in the reaction products was negligibly low for the bipulsing mode. A present limitation is the size of the reaction kettle; however, it should be possible to produce batches containing 100 to 150 g of silicon by scaling up to a larger size kettle.

## ANALYSIS OF SILICON TETRAFLUORIDE BY MASS SPECTROMETRY\*

As a convenient method of rapidly surveying the impurity content in the  $\text{SiF}_4$  used in reaction 1, mass spectrometry was used. Two different samples were analyzed. Sample No. 1 was taken directly from the cylinder supplied by Linde Division, Union Carbide. Sample No. 2 was obtained from the pyrex storage bulb of the reaction system used for the  $\text{Na-SiF}_4$  reaction. From the mass to charge ratio, isotopic distribution, gas beam shutterability, and ionization potential, various mass peaks were assigned to neutral precursors. From the peak intensities, the relative abundance of the various volatile compounds were calculated.

### Experimental

The samples were analyzed by a Nuclide 12-60-HT (12" radius,  $60^\circ$  sector, high temperature source) mass spectrometer. With a 4500-volt ion accelerating potential, ions with a mass-to-charge ratio of up to 1000 can be detected. Ions were produced by electron bombardment in a Nier-Inghram ion source. The ion signal was amplified by an electron multiplier and detected with either a vibrating reed electrometer (VRE), or by counting ion pulses with an Ortec 9315 counter. With this detection system, ion intensities as low as 0.001% of the major peak are normally measured.

The sample gas in a stainless steel reservoir at  $20.0 \pm 0.3$  mm Hg pressure was introduced into the ion source through an orifice (0.013 in. diameter) adjacent to the inlet of the ion source. At the inlet was a

---

\* The work reported in this section was performed by P. Kleinschmidt and D. Hildenbrand.

movable slit which allows one to determine that portion of the signal coming directly from the orifice and that portion due to background gases.

The procedure used for analyzing the sample was to monitor the  $\text{SiF}_3^+$  (major ion of  $\text{SiF}_4$ ) signal and adjust the flow rate until the ion intensity was near the maximum level (that is, at molecular flow conditions and without damaging the detection system). The magnetic field was scanned from a mass to charge ratio of 19 to 370. The ionizing electron energy was set to 20 eV to reduce the extensive fragmentation of  $\text{SiF}_4$  occurring at higher energies. This mass spectrum was then compared with a background mass spectrum. Those masses present in the sample but not in the background were then examined to determine if the signal was shutterable. Also, the flow rate could be regulated with the metering valve. If the signal showed a response to this change in flow rate, we concluded that the signal was caused by molecules in the sample.

## Results

Ions formed from the sample gas were identified from the observed mass numbers, the isotopic distribution, and the threshold appearance potentials. Gaseous impurities positively identified in the sample were  $\text{SO}_2$ ,  $\text{SiOF}_2$ ,  $\text{SO}_2\text{F}_2$ ,  $\text{CCl}_4$ ,  $\text{Si}_2\text{O}_2\text{F}_4$  and  $\text{Si}_2\text{OF}_6$ .

The pressure ratios of all molecules relative to  $\text{SiF}_4$  were calculated from the peak heights of the ion in the mass spectrum. The intensity was corrected for the isotopic distribution and for fragmentation to give the total ion yield of a given molecule at 20 eV. Further corrections were made to the ion intensity to account for the difference in ionization cross sections between  $\text{SiF}_4$  and the impure gases. This correction ranged between 0.7 to 1.9 and was calculated by adding atomic cross sections. The corrected intensities were added and the relative

pressures of the various gases were calculated (see Table 1). No significant difference was detected between the two samples studied.

#### Discussion and Conclusions

In this analysis, impurities with concentrations less than 0.02% were not examined. An unassigned ion was found at mass peak 49. This could be  $\text{BF}_2^+$ . The concentration of this molecule was less than 0.02%. Other unassigned peaks were found at masses 40 and 45.

The principal result of this analysis is that the silicon oxyfluorides are major impurities in commercial  $\text{SiF}_4$ . No evidence was found of phosphorus, titanium, zirconium, vanadium, iron or chromium impurities in concentrations greater than 0.02%. The extensive fragmentation and isotopic spectra of the major impurities, of course, overlapped a substantial portion of the mass spectrum, so that minor impurities at these mass numbers could not be detected. Although volatile impurities of elements such as Ti, V, Zr, Fe, Cr, Al and P in amounts greater than 200 ppm (0.02%) were not detected, this analysis does not preclude their presence in  $\text{SiF}_4$  gas. Methods for detection of low levels of these impurities and their removal from  $\text{SiF}_4$  gas will be investigated.

Table 1

MASS SPECTROMETRIC ANALYSIS OF COMMERCIAL SiF<sub>4</sub>

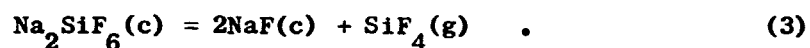
Ion	Mass Number	Intensity (counts per sec)		Neutral Precursor	Relative Abundance pct
		As Recorded	Corrected		
SO <sub>2</sub> <sup>+</sup>	64	20	14	SO <sub>2</sub>	0.035
SiOF <sub>2</sub> <sup>+</sup>	82	37	709	SiOF <sub>2</sub>	1.79
SO <sub>2</sub> F <sub>2</sub> <sup>+</sup>	102	39	39	SO <sub>2</sub> F <sub>2</sub>	0.098
CCl <sub>3</sub> <sup>+</sup>	118	16	63	CCl <sub>4</sub>	0.159
Si <sub>2</sub> O <sub>2</sub> F <sub>4</sub> <sup>+</sup>	164	15	32	Si <sub>2</sub> O <sub>2</sub> F <sub>4</sub>	0.081
Si <sub>2</sub> OF <sub>6</sub> <sup>+</sup>	186	500	1681	Si <sub>2</sub> OF <sub>6</sub>	4.24
SiF <sub>3</sub> <sup>+</sup>	85	33000	37066	SiF <sub>4</sub>	93.6

## ANALYSIS OF SODIUM METAL BY EMISSION SPECTROGRAPHY

Sodium metal used in the  $\text{SiF}_4$ -Na reaction was analyzed by emission spectrography. The only impurities that could be detected were calcium (100 ppm wt), the most commonly found impurity in sodium, and copper (8 ppm wt). However, the analysis indicated that the sodium was quite pure, and it did not contain undesirable impurities such as Ti, V, Zr, Fe, Cr, Mn.

## DISSOCIATION PRESSURE AND THERMODYNAMIC STABILITY OF $\text{Na}_2\text{SiF}_6(\text{c})$ \*

The conditions of temperature and pressure under which  $\text{Na}_2\text{SiF}_6(\text{c})$  is thermodynamically stable are of interest in optimizing the yield of elemental silicon from the reaction of silicon tetrafluoride and sodium, and also for the generation of  $\text{SiF}_4$  by thermal decomposition according to the reverse of the reaction previously indicated as Equation 2, that is,



Optimization of product yield can generally be predicted from standard thermodynamic calculations. However, in the Na-Si-F system, such calculations are precluded by the lack of adequate data on the standard enthalpy of formation,  $\Delta H_{f298}^{\circ}$ , of  $\text{Na}_2\text{SiF}_6(\text{c})$ . There have been several pertinent experimental studies on  $\text{Na}_2\text{SiF}_6(\text{c})$ , including reaction calorimetry<sup>5</sup> and dissociation pressure measurements<sup>6,7</sup> but the results are rather discordant and of uncertain accuracy. The entropy of  $\text{Na}_2\text{SiF}_6(\text{c})$  is known from heat capacity data. From this information, an estimate of

$$\Delta H_{f298}^{\circ}(\text{Na}_2\text{SiF}_6, \text{c}) = -695.4 \text{ kcal/mol}$$

has been derived. Using this result and other available thermochemical data for  $\text{NaF}(\text{c})$ ,<sup>8</sup>  $\text{SiF}_4(\text{g})$ ,<sup>9</sup> and  $\text{Na}_2\text{SiF}_6(\text{c})$ ,<sup>10</sup> one can calculate the equilibrium dissociation pressure for the reaction given in Equation 3 over a wide temperature range. The measured dissociation pressures

---

\* This reaction is based on work performed by D. L. H. Edenbrand, K. H. Lau, and A. Sanjurjo.

scatter widely about the calculated pressures, with the differences amounting to as much as an order of magnitude or more.

Because of these substantial discrepancies, a new determination of the  $\text{Na}_2\text{SiF}_6$  dissociation pressure was initiated at SRI by the torsion-effusion method.<sup>11,12</sup> To date, we have measured the dissociation pressure of commercially obtained\*  $\text{Na}_2\text{SiF}_6$ (s) with two alumina effusion cells having 1.0 and 1.5 mm diameter orifices in the range 585 to 650 K. The results are shown in Figure 7. The slopes of the log P vs. 1/T plots with the two cells are in close agreement, but there is a definite trend such that higher absolute pressures are obtained with the 1.0 mm diameter orifice. This effect is quite common in solid decomposition reactions, and is taken to indicate the existence of a substantial kinetic barrier to the transfer of vaporizing species from a lattice site to the gas phase.<sup>13</sup> It is possible, however, to extrapolate the steady-state pressure data to the zero orifice area, as suggested by a theoretical model of the effusion process,<sup>14,15</sup> and to derive equilibrium pressure from the results. The extrapolated equilibrium pressure data are also shown in Figure 7.

From least squares fitting, the following expressions for the dissociation pressure were obtained:

$$\text{1.0 mm diam. orifice: } \log P(\text{atm}) = (9.31 \pm 0.11) - (9180 \pm 70)/T$$

$$\text{1.5 mm diam. orifice: } \log P(\text{atm}) = (9.55 \pm 0.43) - (9440 \pm 27)/T$$

The corresponding equation for the extrapolated equilibrium pressure is  $\log P_{\text{eq}}(\text{atm}) = 9.11 - (9180/T)$ .

It is assumed that the observed dissociation process is given by Equation 3, but this will be checked by determining the molecular weight

---

\* 99%  $\text{Na}_2\text{SiF}_6$  obtained from Ventron Corporation, Massachusetts.

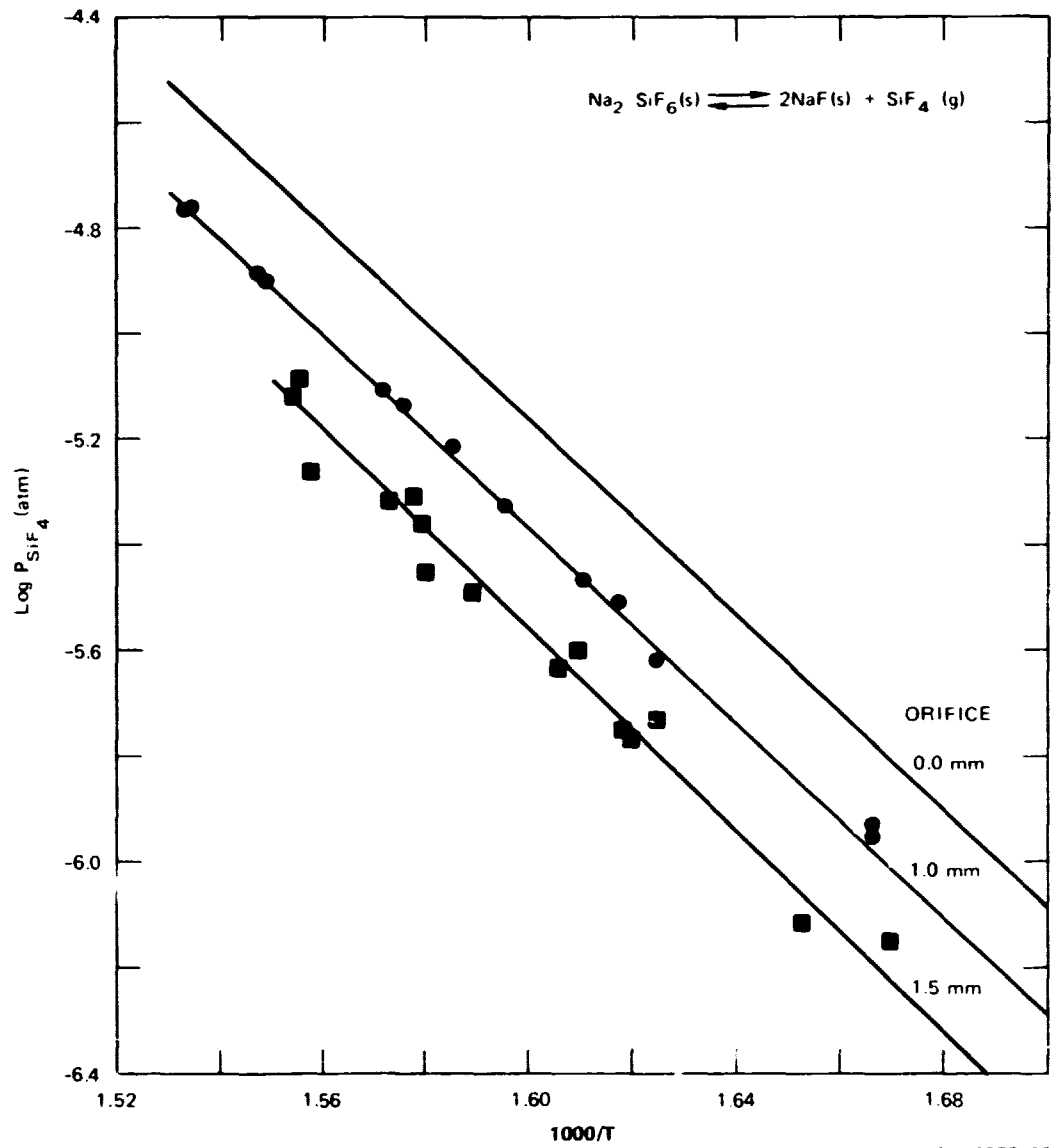


FIGURE 7 TORSION EFFUSION MEASUREMENTS OF  $\text{P}_{\text{SiF}_4}$

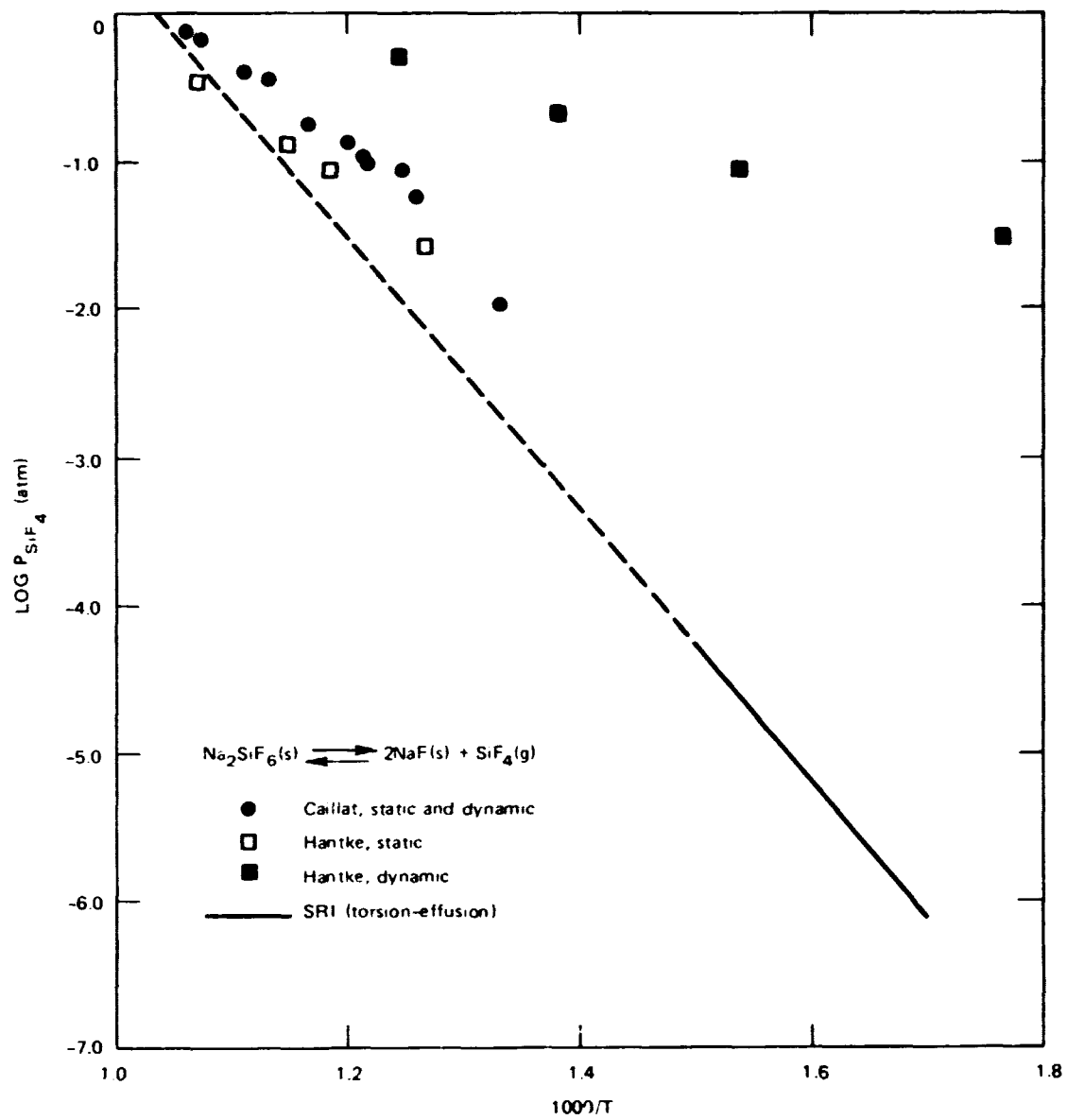
of the effusing vapor from simultaneous torque-angle and weight-loss measurements.

Examination of the cell residues by x-ray diffraction showed the presence of  $\text{Na}_2\text{SiF}_6(\text{s})$  and  $\text{NaF}(\text{s})$  only, so that the decomposition process appears to be correct as written in Equation 3. In particular, there was no evidence of additional compounds such as  $(\text{NaF}\cdot 4\text{Na}_2\text{SiF}_4)$ , the presence of which would substantially alter the interpretation.

The second law slopes of the dissociation pressure data (that is slopes of the plots of  $\log P$  vs.  $1/T$  yield values of 42.0 and 32.2 kcal/mol for the enthalpy change of the decomposition process at the average temperature of the measurements, using the 1.0 and 1.5 mm diam. orifices, respectively.

Data obtained with the smaller effusion orifice are believed to be the more reliable because of the higher precision. The slope heat of 42.0 kcal/mol can be combined with heat capacity data to yield  $\Delta H_{298}^{\circ} = 44.0$  kcal/mol for the decomposition reaction (Equation 3). A preliminary third law calculation, based on the absolute pressure and estimated entropy for  $\text{Na}_2\text{SiF}_6(\text{c})$  yields  $\Delta H_{298}^{\circ} = 40.4$  kcal/mol. The  $\Delta H_{298}^{\circ}$  values calculated by the second law and the third law differ by 3.6 kcal/mol. However, the effusion data show  $\text{Na}_2\text{SiF}_6(\text{c})$  to have a significantly higher thermodynamic stability than indicated by previous data. ( $\Delta H_{298}^{\circ} = 36.4$  kcal/mol.)<sup>5</sup> Measured dissociation pressures are two orders of magnitude less than values calculated from NBS data.<sup>8</sup>

In Figure 8, the equilibrium pressures derived from the effusion studies are plotted along with the data of Hantke<sup>6</sup> and Caillat<sup>7</sup> obtained at higher temperatures. The literature data are quite scattered, but the extrapolation of SRI effusion data appears consistent with them at the highest temperatures.



SA-4980-21

FIGURE 8 EQUILIBRIUM PRESSURE OF  $\text{SiF}_4$  VERSUS TEMPERATURE

According to the presently obtained extrapolated relation for the pressure of  $\text{SiF}_4$  in Equation 3, an equilibrium pressure of 1 atm of  $\text{SiF}_4$  should be reached at  $734^\circ\text{C}$ . For a dynamic system, Yaws et al<sup>12</sup> have shown that  $\text{Na}_2\text{SiF}_6$  dissociates rapidly and completely at  $600^\circ\text{C}$ , the highest temperature studied. Further studies at SRI will concentrate on the temperature region  $350\text{--}700^\circ\text{C}$ .

#### FUTURE WORK

During the next quarter, we intend to study the leaching process in further detail in order to establish the most suitable conditions for separating silicon from the reaction products NaF and  $\text{Na}_2\text{SiF}_6$ . We also plan to examine candidate methods for the preparation of  $\text{SiF}_4$  gas from commercially obtained  $\text{H}_2\text{SiF}_6$  (aq). Our objective will be to select the most suitable process for obtaining pure  $\text{SiF}_4$  gas from  $\text{H}_2\text{SiF}_6$  economically.

#### REFERENCES

1. V. K. Kapur and L. Nanis, "Novel Duplex Vapor Electrochemical Method for Silicon Solar Cells," Quarterly Report No. 1 (August 1976).
2. V. K. Kapur and L. Nanis, "Novel Duplex Vapor Electrochemical Method for Silicon Solar Cells," Quarterly Report Nos. 2 and 3 (November 1976).
3. See reference 1 page 9.
4. See reference 2 page 7.
5. A. F. Vorob'ev et al., Russ J. Inorg. Chem. 5, 681 (1960).
6. G. Hantke, Angew. Chem. 39, 1065 (1926).
7. R. Caillat, Ann. Chim. (France) 20, 367 (1945).
8. D. D. Wagman et al., "National Bureau of Standards Report," NBSIR 76-1034 (April 1976).
9. JANAF Thermochemical Tables, NSRDS-NBS 37, 2nd Ed., U.S. Govt. Printing Office, Washington, D.C. (1971).
10. D. R. Stull et al., J. Chem. Eng. Data 15, 52 (1970).
11. D. L. Hildenbrand and W. F. Hall, J. Phys. Chem. 67, 888 (1963).
12. D. L. Hildenbrand and D. T. Knight, J. Chem. Phys. 51, 1260 (1969).
13. K. H. Lau, D. Cubicciotti and D. L. Hildenbrand, J. Chem. Phys. 66, 4532 (1977).
14. C. I. Whitman, J. Chem. Phys. 29, 161 (1952).
15. K. Motzfeldt, J. Phys. Chem. 59, 139 (1955).
16. K. C. Hansen, J. R. Hopper, J. W. Miller, C. L. Yaws, Quarterly Report ERDA/JPL 954343-76/1.